THE ASTROPHYSICAL JOURNAL, 493:950–954, 1998 February 1

FIRST ASTRONOMICAL IMAGES SHARPENED WITH ADAPTIVE OPTICS USING A SODIUM LASER GUIDE STAR

M. LLOYD-HART, J. R. P. ANGEL, T. D. GROESBECK, T. MARTINEZ, B. P. JACOBSEN, B. A. MCLEOD,[1]
D. W. MCCARTHY, E. J. HOOPER, E. K. HEGE, AND D. G. SANDLER[2]
Center for Astronomical Adaptive Optics, University of Arizona, Tucson, AZ 85721
Received 1997 June 25; accepted 1997 September 10

ABSTRACT

Adaptive optics with a sodium resonance laser guide star was used at the Multiple Mirror Telescope (MMT) in 1996 April to image the core of the globular cluster M13 (NGC 6205). A 23″ field was recorded in the K_s band with image resolution of 0.″51, when the uncorrected resolution was 0.″72. Global tilt, not sensed by the laser, was measured from the image motion of a star 35″ from the center of the field. Despite this separation, the star profiles do not vary significantly across the image. Many more stars fainter than $K_s = 17.5$ can be identified in the corrected image.

The 0.″5 imaging capability demonstrated here, though not reaching the performance of existing faster, higher order systems with natural star wave-front sensors, is significant because it can be generally realized for very faint objects under normal observing conditions. This characteristic will carry over to higher order laser-based systems, making them very powerful. Our current 0.″5 resolution is much larger than the diffraction limit for the present MMT array (and its upcoming 6.5 m monolithic replacement) because discontinuities prevent the measurement of phase differences between the array elements. Furthermore, small-scale wave-front aberrations caused by atmospheric and static errors across individual mirrors were not corrected. But our system, by its simultaneous correction of differential slopes derived from the laser beacon and global tilt from the natural guide star, illuminates the principles and sources of error common to all future laser systems.

Subject headings: atmospheric effects — methods: observational — techniques: image processing — telescopes — turbulence

1. INTRODUCTION

Current adaptive optics (AO) systems rely on relatively bright natural field stars to measure phase errors, which limits their operation to only a few percent of the sky (Roddier et al. 1995; Léna 1996; Brandl et al. 1996). This constraint should be largely overcome for infrared imaging with large telescopes when laser-generated artificial stars or "beacons" are used to measure wave-front errors (Sandler et al. 1994a). Fugate et al. (1991) has used a 1.5 m telescope with a closed-loop AO system to recover images near the diffraction limit, relying on a beacon at 10–20 km altitude produced by Rayleigh scattering. Correction of large telescopes requires a higher altitude beacon. Happer & MacDonald (1983) and Foy & Labeyrie (1985) have proposed a beacon taking advantage of resonant scattering in the mesospheric sodium layer at ~95 km. Laser systems to create such stars at the 589 nm D2 line have been tested by Fugate et al. (1991), and more recently by Kibblewhite (1992), Lloyd-Hart et al. (1995), and Olivier et al. (1995).

Because the outbound laser beam jitters in an unknown way, the lowest order atmospheric aberration, which causes global image motion, is not sensed by the beacon. A natural star is therefore still required to sense this motion. Nonetheless, the laser beacon provides a great advantage by allowing much better sky coverage. Since only two parameters need be measured from the natural star, given by its motion, very faint field stars suffice.

In this paper, we report the first practical application of an AO system using a sodium resonance beacon. The low-order AO system (Gray et al. 1995) at the Multiple Mirror Telescope (MMT), which corrects wave-front tilt errors across the individual primary mirrors, has been used to obtain compensated images of the nearby globular cluster M13 (NGC 6205). Signals from the laser guide star were used to sense differential slopes between the six apertures, while global motion was independently measured with a faint natural guide star.

Under typical observing conditions, instantaneous K-band images from the individual telescopes often show a nearly diffraction-limited core of 0.″3 containing ~40% of the total energy. This is consistent with the known telescope aberrations and measurements of Fried's coherence length r_0 of typically 0.9 m, half the current individual mirror diameter of 1.8 m. By correcting the wave-front tilt over each of the apertures, the sharp core can, in principle, be recovered in a long-exposure image with the full telescope.

2. HARDWARE DESCRIPTION

2.1. *Cassegrain Instrument*

Figure 1 shows a schematic view of our instrument. Light from the six separate Cassegrain telescopes is reflected to the central beam-combining pyramid (Close et al. 1995) by tertiary mirrors. The pyramid directs light off rapidly steerable facets to a pseudo-Cassegrain f/8.4 focus where the six fields are made coincident. Wavelengths longer than 1 μm are transmitted by a dichroic beam splitter near the focal plane, which forms the entrance window of the science Dewar containing a 256 × 256 NICMOS3 array. Reimaging optics in the Dewar provide a pixel scale of 0.″090, giving a field of view of 23″.

[1] Harvard-Smithsonian Center for Astrophysics, 60 Garden Street, Cambridge, MA 02138.
[2] ThermoTrex Corporation, 10455 Pacific Center Court, San Diego, CA 92121; mhart@as.arizona.edu.

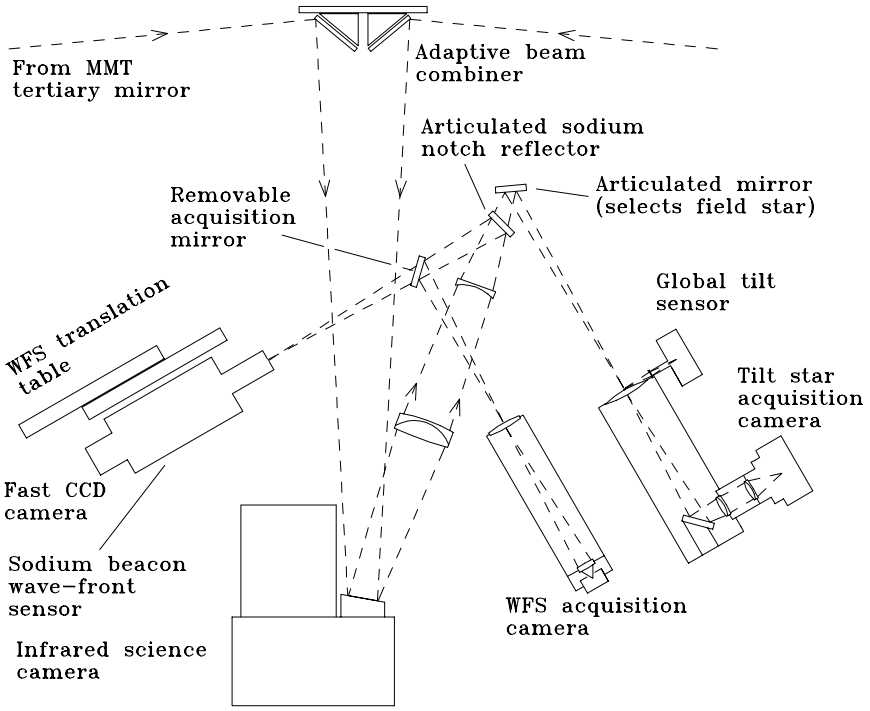

FIG. 1.—Schematic view of the Cassegrain instrument. After correction at the adaptive beam combiner, infrared light is brought straight into the science Dewar to a NICMOS3 array, while visible light is reflected upward to the wave front sensing portion of the instrument. Laser light is reflected to the wave-front sensor; light from natural field stars is sent via a steerable mirror to the global tilt sensor.

Visible light is reflected upward through a relay lens to an articulated mirror that can direct any selected portion of a 4′ field to the Shack-Hartman wave-front sensor (WFS). This mirror is precisely located at the pupil formed by the relay, so that the pupil reimaged onto the lenslet array in the WFS remains well aligned. A lens before the WFS places the entrance pupil at infinity, so that continuous translation of the WFS to maintain focus on the sodium layer (whose distance is a function of elevation) leaves the pupil still in focus on the lenslets. The CCD pixel scale is chosen so that when the wave front is unaberrated, each image is centered at the intersection of 4 pixels. The adaptive control servo moves the beam-combiner facets to make the four signals equal in each "quad cell," thus keeping the six images at the focal plane in coincidence.

For operation with the laser, the sodium guide star is reflected to the WFS by a dielectric notch reflector centered at 589 nm in place of the articulated pupil mirror. Other wavelengths are transmitted to a second articulated mirror, which directs light from a chosen field star to the global tilt sensor at a combined focal plane. The tilt sensor is another fast-scanned CCD array, operated as a single quad cell. Its measure of overall tilt is added to the signals from the WFS in the computer, which applies corrections to the beam-combiner facets.

2.2. *Sodium Laser and Beam Projector*

For the present experiment, the beacon was generated by a continuous-wave laser beam. The standing-wave laser uses rhodamine 6G dye pumped by a 25 W argon ion laser. About 3.2 W was developed at the sodium D2 line, of which 1.8 W was transmitted through the beam projector to the sky. The beam expander is a refractor with 48 cm diameter aperture, mounted close to the optical axis of the MMT array (Jacobsen et al. 1994). The beam had an elliptical Gaussian profile of 18 × 12 cm FWHM and was focused to produce the smallest obtainable illuminated spot at the sodium layer. For the present experiments, the sodium guide star image recorded at the WFS had a FWHM of 1″.1. The beacon appeared as bright as a star of $R \sim 10$ seen through an R filter.

3. OBSERVATIONS OF M13

As a test of the laser system, we have obtained images of a rich field in the core of the nearby globular cluster M13. Figure 2 (Plate 47) shows two exposures taken in the K_s band with and without adaptive compensation by the laser beacon and natural tilt star. Corrections to both differential and global tilt were applied at 30 Hz. The image is centered on coordinates $\alpha = 16^h41^m39^s.9$, $\delta = 36°27'26''.1$ (J2000).

The uncompensated image in Figure 2*a* was derived by combining three consecutive 20 s exposures. The point-spread function (PSF) has a FWHM of 0″.72, which indicates that observing conditions at the time were close to median for the site. Analysis of image motion in frames recorded simultaneously by the WFS shows that r_0 was 85 cm at 2.2 μm. The compensated image is shown in Figure 2*b*, again the result of combining three 20 s exposures. For this image, the laser guide star was placed at the center of the field of view (the beam is of course invisible to the infrared camera) and global tilt information was derived from a natural star ($V \approx 12.7$) separated from the laser by 35″, outside the field of view to the northeast. The mean FWHM of the stellar profiles in the image with AO correction is 0″.51. The reduction in width is accompanied by an improvement in the Strehl ratio or peak brightness of 1.7.

To be sure that the improvement is due to correction of atmospheric motion rather than alignment errors, the

uncorrected image was observed immediately after the AO system had been run. The beam-combiner tilts were each set equal to their average value during adaptive correction. The measured optomechanical instabilities of the telescope are slow enough ($\sim 0''.03$ per minute) that they do not contribute significantly to blurring of the uncorrected image.

The scientific value of the adaptive image sharpening is illustrated by the improvement in the limiting magnitude in this confusion-limited region. We first processed both corrected and uncorrected images with the iterative blind deconvolution algorithm (Jefferies & Christou 1993), to make detection of fainter objects more straightforward. We then used the DAOPHOT package (Stetson 1987) under IRAF to derive photometry. The observed luminosity functions are plotted in Figure 3. The total number of detections increased from 109 in the uncorrected image to 151 in the compensated image. In particular, the number of faint star detections was much greater for the image with AO correction. In this image, 51 stars fainter than $K_s = 17.5$ were found, compared to nine in the image without AO.

The result of the deconvolution of the AO corrected image is shown in Figure 2*c*, which has a mean FWHM for the stellar images of $0''.36$. The reality of the additional faint stars has been checked by comparison with V-band images of M13 obtained with the WF/PC–1 camera of the *Hubble Space Telescope* (*HST*) (Cohen et al. 1997). We show the positions of stars identified by *HST*, to a limiting magnitude of $V = 19$, as dots overlaid on the deconvolved image of Figure 2*c*. Of the 51 faint stars found, all but three are coincident with a star from the *HST* image. The photometry performed on this image has been used in conjunction with additional data from the MMT AO system and the *HST* data to obtain color-magnitude diagrams for our observed field. These results will be presented in a separate paper.

The reason for the improved detection of faint stars can be seen in the modulation transfer functions of the uncorrected and AO corrected images, as shown in Figure 4. Although the throughput of high spatial frequencies with adaptive correction does not approach the diffraction-limited case, an enhancement is apparent, approaching a factor of 2 at the high-frequency end.

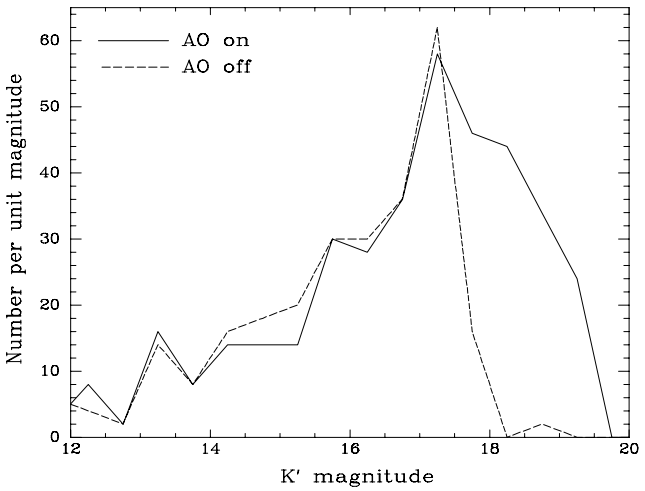

FIG. 3.—Observed stellar luminosity functions derived from the corrected and uncorrected images of Fig. 2, after deconvolution. The bins in this plot are 0.5 mag wide. The drop beyond magnitude 17 is caused by incompleteness. With adaptive optics however, many more stars are observable in the incompletely sampled range from $K_s = 17.5$ to 19.5.

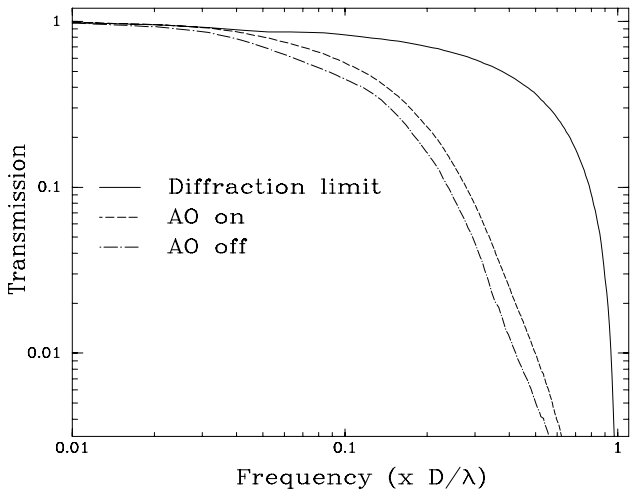

FIG. 4.—Modulation transfer functions measured from the images of Figs. 2*a* and 2*b*, compared to the theoretical curve for a diffraction-limited aperture of 1.83 m diameter. Although we do not reach the diffraction limit with adaptive optics, the throughput of high spatial frequencies ($0.2–0.5 \times D/\lambda$) is improved by a factor of ~ 2.

4. EXPERIMENTAL EVALUATION OF SOURCES OF RESIDUAL ERROR

While the corrected image of M13 shows significant improvement, the star profiles are not reduced to the instantaneous single telescope limit of $\sim 0''.3$. The PSF is degraded by residual wave-front aberration arising from a number of sources. To distinguish and understand these errors, we consider here the results of some simpler closed-loop experiments with wave-front measurements from natural stars. We rely on the results of the error analysis for laser guide star adaptive optics given by Sandler et al. (1994a) and the characterization of the atmospheric aberration at the MMT site by Lloyd-Hart et al. (1995). We estimate the different errors in terms of their contribution to the wave-front phase error in radians at 2.2 μm wavelength.

The experiments were not all performed on the same night. Although the observing conditions were approximately the same in all cases (as measured by the FWHM of long-exposure uncorrected images), they were not identical, and so the results must be considered approximate.

In the simplest case, long-exposure K-band images of a 10th magnitude star were taken singly with each aperture of the MMT array, corrected for image motion at a rate of 90 Hz. The resulting six images had a mean FWHM of $0''.35$. The image degradation beyond the diffraction limit of $0''.25$ arises largely from higher order wave-front errors, rather than tilt. Spatial errors are caused mostly by atmospheric wave-front curvature that remains uncorrected across the primary mirrors (fitting error) and fixed aberrations in the telescopes themselves. We estimate the fitting error to be ~ 0.7 rad rms and the fixed optical aberrations to be ~ 1.0 rad rms. Further error arises from the time delay in the servo loop; from earlier measurements of the temporal coherence of the turbulence (Lloyd-Hart et al. 1995), we expect a contribution of 0.5 rad rms. An additional contribution from the combined photon and read noise of the wave-front sensor array is estimated at about 0.25 rad rms.

Added in quadrature, these errors total ~1.3 rad rms, for an expected Strehl ratio of 0.28. Since most of this wave-front error is on rather small scales, the bulk of the light scattered out of the image core appears in an underlying broad halo. The PSF profile is thus distinctly non-Gaussian, with a sharper FWHM than a Gaussian image of the same total intensity.

In the second experiment adaptive correction was made of the full aperture, from natural star wave-front measurements. The guide star was Gliese 229A, an M1 dwarf with R magnitude 7.9. The corrected image of the star and the field around it was recorded in a 60 s K-band exposure (Fig. 5). The brown dwarf companion at 7″ separation (Nakajima et al. 1995) is seen with a resolution of 0.″45 FWHM. The image degradation that has largely removed the 0.″35 core seen in the first experiment is due to static errors in the automatic registration of the six wave-front tilts. Coma-like aberrations seen in the telescope optics account for this. The centroid of the visible guide star image found by the WFS is displaced from the instantaneous infrared diffraction core when the wave front is asymmetrically distorted. This effect accounts for offsets measured at typically 0.″07 from the axis.

The further increment to 0.″51 seen in the laser-guided image of M13 corresponds to a width of 0.″24 added in quadrature. The fundamental sources of additional error in the laser guide star mode, from focus anisoplanatism in the sodium guide star wave front (0.12 rad rms; Lloyd-Hart et al. 1995) and tilt anisoplanatism for the off-axis guide star (see below), are small. The dominant source of the observed additional error is an increase in the servo lag error to 1.5 rad rms because of the slower correction rate of 30 Hz, adopted to reduce noise in the guide star tilt measurements. There are also small additional noise contributions from the global tilt sensor and the WFS measurements because the laser beacon image is not as sharp as the image of a natural guide star.

We have looked for evidence of tilt anisoplanatism in the corrected image of M13, but there appears to be no correlation of image size with radial distance from the tilt star. This is to be expected on the basis of previous explicit measurements of anisoplanatism using binary stars (Lloyd-Hart et al. 1995). Over the range 20–45″, corresponding to the separations of the stars in the field of Figure 2 from the tilt star, one would expect anisoplanatism to contribute 0.″02–0.″05 to the width of the PSF. When added in quadrature to the axial PSF, already at 0.″5, the difference in these values becomes immeasurably small.

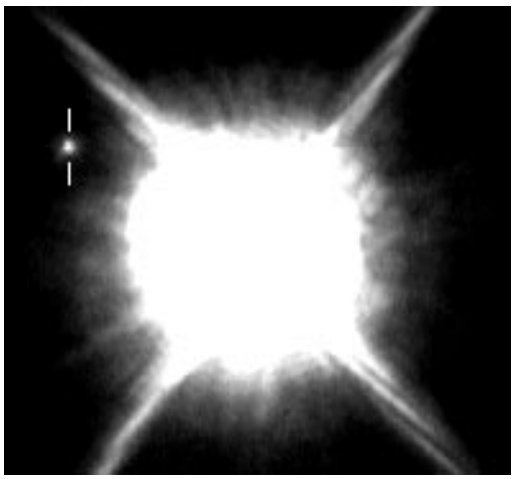

FIG. 5.—K-band image of the Gl 229 system. For this 60 s exposure, wave-front tilts over the six MMT segments were corrected using visible light from the bright primary star, badly saturated in this image. The image of the faint companion, 7″ away, appears with FWHM of 0.″45 at a SNR of 12,500.

5. DISCUSSION AND CONCLUSIONS

5.1. *Sky Access with the Present System*

We have demonstrated a sodium laser guide star system that gives a useful improvement in resolution to 0.″5 in the K band. Since the laser guide star can be created anywhere on the sky, the limit to applicability is set by the need for a faint natural guide star for global tilt measurement. The guide star used for global tilt correction for M13 was brighter than necessary, $V = 12.7$, contributing a tilt measurement error of only 0.″02. We estimate from the measured instrument throughput and detector noise that the limiting magnitude for 0.″1 measurement accuracy is $R \approx 16.7$. The density of field stars this bright or brighter at mid–Galactic latitudes is about 1000 per square degree (Bahcall & Soneira 1981). Thus the probability of finding one or more within 1′ of any object is about 50%. Tilt anisoplanatism is ~0.″1 at this angular separation (Lloyd-Hart et al. 1995). Thus the additional combined error ~0.″15 is small compared to the system resolution of 0.″5, and imaging to this resolution is possible with probability ~50% for any object.

5.2. *Extension to the* 6.5 m *Converted MMT*

Next year the MMT will be converted to operation with a single 6.5 m primary mirror (West 1996) and a sodium laser adaptive optics system (Lloyd-Hart et al. 1996). Performance to the full aperture K-band diffraction limit is targeted. The present experiment provides many insights because it parallels closely the method needed for full wave front recovery.

An important aspect underscored by the present system is the difficulty of finding adequate global tilt guide stars at visible wavelengths. To avoid increasing the 6.5 m diffraction-limited image of 0.″07 FWHM by more than 10%, it must be stabilized to an rms motion of ~0.″03. The present system would require a natural star of $R \sim 14$ to achieve this accuracy, and the probability of finding such a star is small. The problem is exacerbated by the smaller allowable angular separation of ~35″ permitted by anisoplanatism (Lloyd-Hart et al. 1995).

The solution is to measure global motion in the near-infrared, where the photon flux of field stars is typically stronger but, more importantly, one can take advantage of sharper images. Measurements of the correlation of the wave front with field angle (Lloyd-Hart et al. 1995) show that in the infrared, field stars will be corrected by the laser almost to the diffraction limit (Sandler et al. 1994a) for angles of up to ~30″. The corresponding error reduction compared to sensing with ten times larger seeing-limited images in the visible is equivalent to a 100 times increase in photon flux.

For the 6.5 m system, we plan to use a portion of a slow-scanned NICMOS3 HgCdTe array as the sensor, which can achieve readout noise as low as 5 e rms. Using a plate scale of 0.″15 per pixel, sky background will be

reduced to magnitude 19 per pixel, and the limiting magnitude for the sensor will be $H \sim 18$ (Sandler et al. 1994b). From the results of Bahcall & Soneira (1981) and Wainscoat et al. (1992), we compute that, averaged over all Galactic latitudes, the 6.5 m system will have access to 65% of the sky.

This work has been supported by the Air Force Office of Scientific Research under grant F49620-94-100437. E. K. H. thanks E. M. Hege and the University of Arizona Foundation for support of the iterative deconvolution image calibration. Many thanks to E. Olszewski for assistance with the photometric data reduction. We are very grateful to the staff of the MMT for their support in this most demanding work. Observations reported here were made at the Multiple Mirror Telescope Observatory, a joint facility of the University of Arizona and the Smithsonian Astrophysical Observatory.

REFERENCES

Bahcall, J. N., & Soneira, R. M. 1981, ApJS, 47, 357
Brandl, B., et al. 1996, in Proc. ESO/OSA Topical Meeting on Adaptive Optics, ed. M. Cullum, (Garching: ESO), 521
Close, L. M., Brusa, G., Bruns, D. G., Lloyd-Hart, M., & McCarthy, D. W. 1995, Proc. SPIE, 2534, 105
Cohen, R. L., Guhathakurta, P., Yanny, B., Schneider, D. P., and Bahcall, J. N. 1997, AJ, 113, 669
Foy, R., & Labeyrie, A. 1985, A&A 152, 129
Fugate, R. Q., et al. 1991, Nature, 353, 144
Gray, P. M., et al. 1995, Proc. SPIE, 2534, 2
Happer, W., & MacDonald, G. J. 1983, MITRE Corp., McLean, VA, JASON Report JSR-82-106
Jacobsen, B. P., et al. 1994, Proc. SPIE, 2201, 342
Jefferies, S. M., & Christou, J. C. 1993, ApJ, 415, 862
Kibblewhite, E. J. 1992, in Proc. Laser Guide Star Adaptive Optics Workshop, ed. R. Q. Fugate (Albuquerque: Phillips Lab.), 24
Léna, P. 1996, in Proc. ESO/OSA Topical Meeting on Adaptive Optics, ed. M. Cullum, (Garching: ESO), 317
Lloyd-Hart, M., et al. 1995, ApJ, 439, 455
Lloyd-Hart, M., Angel, J. R. P., Sandler, D. G., Groesbeck, T. D., Martinez, T., & Jacobsen, B. P. 1996, Proc. SPIE, 2871, 880
Nakajima, T. Oppenheimer, B. R., Kulkarni, S. R., Golimowski, D. A., Matthews, K., & Durrance, S. T. 1995, Nature, 378, 463
Olivier, S. S., et al. 1995, in Proc. ESO/OSA Topical Meeting on Adaptive Optics, ed. M. Cullum, (Garching: ESO), 75
Roddier, F., et al. 1995, ApJ, 443, 249
Sandler, D. G., Stahl, S., Angel, J. R. P., Lloyd-Hart, M., & McCarthy, D. W. 1994a, J. Opt. Soc. Am. A, 11, 925
Sandler, D. G., Stahl, S., Angel, J. R. P., & Lloyd-Hart, M. 1994b, Proc. SPIE, 2201, 407
Stetson, P. B. 1987, PASP, 99, 191
Wainscoat, R. J., Cohen, M., Volk, K., Walker, H. J., & Schwartz, D. E. 1992, ApJS, 83, 111
West, S. C. 1996, Proc. SPIE, 2871, 38

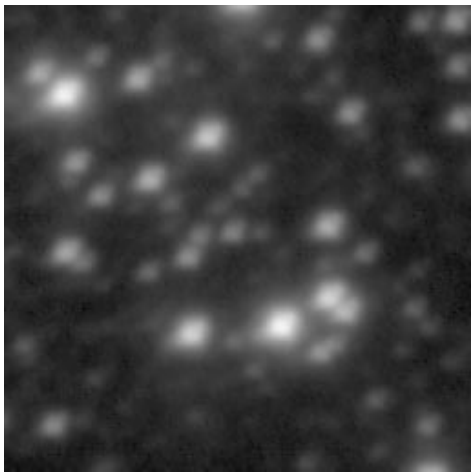

FIG. 2*a*

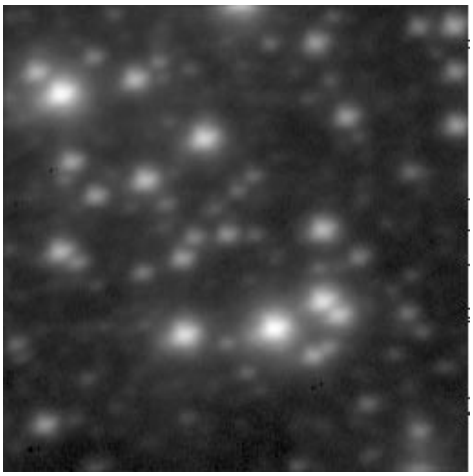

FIG. 2*b*

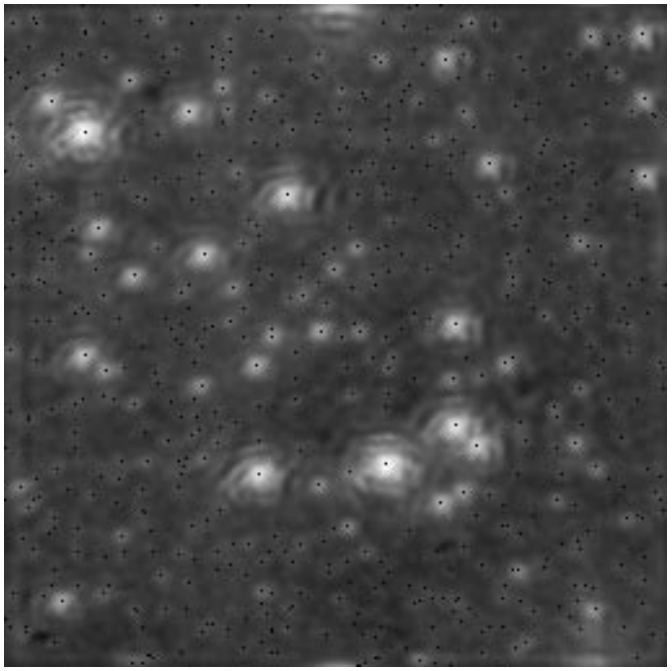

FIG. 2*c*

FIG. 2.—K_s-band images before and after correction with the adaptive optics system, using a sodium laser beacon as the wave-front reference source. (*a*) With no correction, the stellar images are seeing limited at 0".72 in a 60 s exposure. (*b*) With correction on the basis of the sodium laser beacon, and global image motion corrected by reference to a natural star, the images in this 60 s exposure have been improved to 0".51. (*c*) After PSF subtraction using the iterative blind deconvolution algorithm on the corrected image, the image size is further improved to 0".36. The positions of 570 stars from a *V*-band image from the HST's WF/PC-1 camera are superposed as dots. All images are shown on a logarithmic gray scale to give a dynamic range of 1000, while exaggerating the halos of the bright stars. North is approximately 15° clockwise from vertical; east is to the left.

LLOYD-HART et al. (see 493, 951)